

# Electric-Energy Generation Using Variable-Capacitive Resonator for Power-Free LSI: Efficiency Analysis and Fundamental Experiment

Masayuki Miyazaki, Hidetoshi Tanaka, Goichi Ono, Tomohiro Nagano\*, Norio Ohkubo, Takayuki Kawahara, and Kazuo Yano

Hitachi Lt d., Central Research Laboratory, Kokubunji, Tokyo, JAPAN

\*Hitachi ULSI Systems, Co. Ltd., Kokubunji, Tokyo, JAPAN

Phone: +81-42-323-1111

mmya@crl.hitachi.co.jp

## ABSTRACT

A power generator based on a vibration-to-electric energy converter using a variable-resonating capacitor is experimentally demonstrated. The generator consists of a complete system with a mechanical-variable capacitor, a charge-transporting LC tank circuit and an externally powered timing-capture controller. A practical design methodology to maximize the efficiency of the vibration-to-electric energy generation system is also described. The efficiency of the generator is estimated based on three factors: the mechanical-energy loss, the charge-transportation loss, and the timing-capture loss. Through the mechanical-energy analysis, the optimum condition for the resonance is found. The parasitic elements in the charge transporter and the timing management of the capture scheme dominate the generation efficiency. These analyses enable the optimum design of the energy-generation system. An experimentally fabricated

and measured generator theoretically has a maximum power of 580 nW; the measured power is 120 nW, so conversion efficiency is 21%. This results from a 43% mechanical-energy loss and a 63% charge-transportation loss. The timing-capture scheme is manually determined and externally powered in the experiment, so its efficiency is not considered. With our result, a new system LSI application with an embedded power source can be explored for the ubiquitous computing era.

## Categories and Subject Descriptors

C3 [Computer Systems Organization]: Special-purpose and Application-based Systems – *real-time and embedded systems*.

## General Terms

Design

## Keywords

Vibration energy, resonance, variable capacitance, power generation.

## 1. INTRODUCTION

The power consumption of the system LSI in mobile-computing devices continues to be reduced, expanding the battery lifetime of such devices. In the

Permission to make digital or hard copies of all or part of this work for personal or classroom use is granted without fee provided that copies are not made or distributed for profit or commercial advantage and that copies bear this notice and the full citation on the first page. To copy otherwise, or republish, to post on servers or to redistribute to lists, requires prior specific permission and/or a fee.

ISLPED '03, August 25-27, 2003, Seoul, Korea.

Copyright 2003 ACM 1-58113-682-X/03/0008...\$5.00.

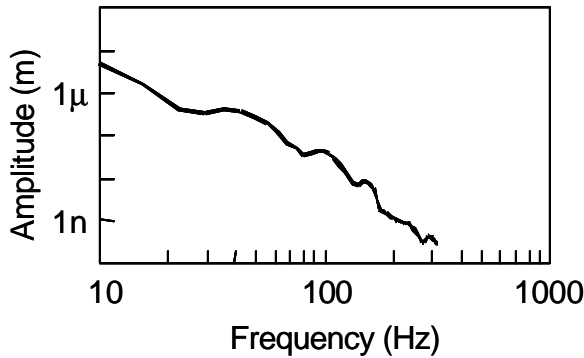


Fig. 1 Measured ambient vibration of a building wall

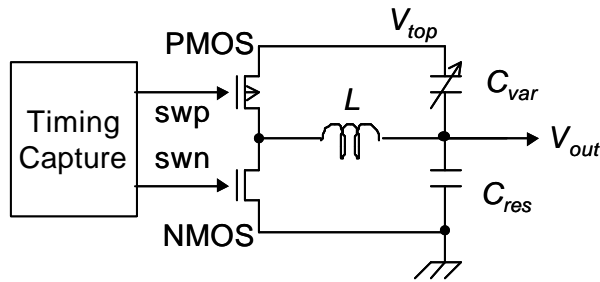


Fig. 2 Vibration-to-electric energy converter

coming ubiquitous computing era, power-free LSIs, i.e. battery-free systems, are desirable because LSI chips will be distributed throughout our surroundings. Therefore, an ambient-energy scavenging or harvesting technology will be required. Such a technology would enable a power source to be embedded on a chip as a functional module. The most possible energy source is a small vibration in the environment. The measured vibration of the wall of a building is shown in Fig. 1. It shows that there is a small but constant vibration. It would be useful if such vibration energy could be scavenged because such energy exists everywhere. Converting vibration energy into electrical energy can be done using three types of devices: a variable capacitor, an electromagnetic inductor, and a piezoelectric transducer. A variable capacitor is the easiest to fabricate because a conventional CMOS process can be used. A charge-pump circuit has been experimentally shown to be a way to use a variable capacitor [1]. However, the system does not generate power by itself. A study has shown that

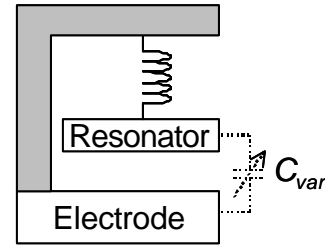


Fig. 3 Variable capacitor

self-sustained power generation using ambient vibration is feasible [2], and a conceptual system of the generator has been presented [3]. However, a stand-alone energy converter with a variable capacitor has not yet been experimentally demonstrated. We have analyzed the energy-conversion efficiency in the generator and have identified an optimum design methodology. Fundamental energy-generation experiment on a vibration-to-electric energy converter using a variable-capacitive resonator demonstrates that it has an efficiency of 21%.

## 2. PRINCIPLE OF ENERGY CONVERSION

The vibration-to-electric energy converter is shown in Fig. 2 [3]. Variable capacitor  $C_{var}$  resonates due to externally forced vibration. It is composed of a resonator and an electrode, as shown in Fig. 3. When the electrode is set on a wall, for instance, it picks up the vibration and resonates. As a result, the capacitance between the resonator and the electrode varies cyclically.

The energy-conversion process is as follows. First, an initial charge,  $q_0$ , is supplied to the output,  $V_{out}$ . When the capacitance  $C_{var}$  reaches a maximum, the timing-capture scheme switches on the NMOS and PMOS transistors in turn to carry the charge from  $V_{out}$  to the node,  $V_{top}$ . The capacitance  $C_{var}$  then drops from the maximum to the minimum. The timing-capture scheme then switches on the PMOS and NMOS transistors in turn to carry the charge back to  $V_{out}$ . During this process, the charged resonator works against the Coulomb force; this workload corresponds to generated energy. The resonance behavior is analyzed using a dynamic equation:

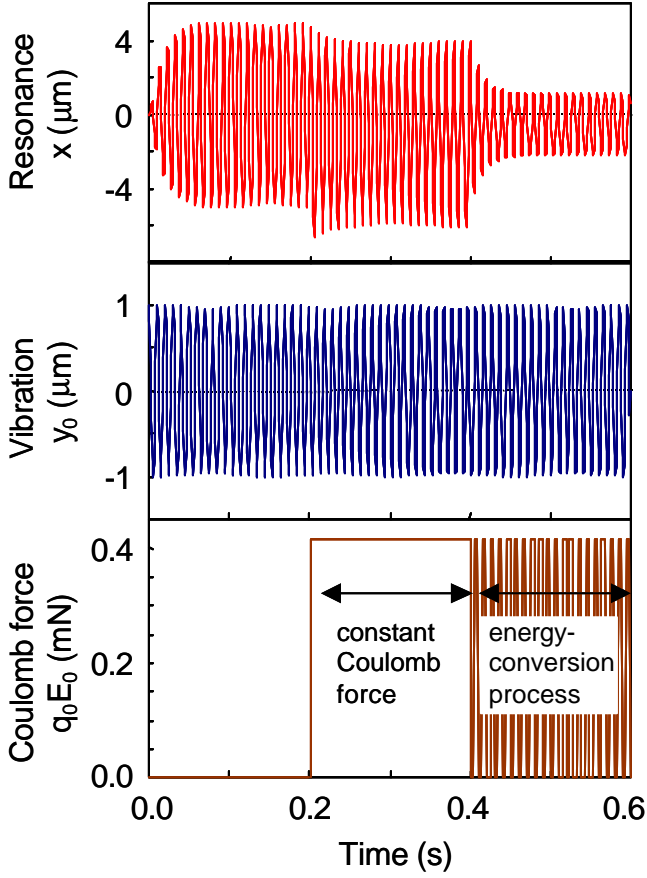


Fig. 4 Resonance behavior under conditions of vibration and Coulomb force

$$m\ddot{x} + c\dot{x} + kx = ky_0 \cdot \cos(2\mathbf{p} \cdot f_0 t) - q_0 E_0, \quad (1)$$

where  $m$  is the mass of the resonator,  $c$  is the damping coefficient,  $k$  is the spring constant, and  $f_0$  is the resonance frequency. The term  $ky_0$  represents the external vibration, and  $q_0 E_0$  represents the Coulomb force.

The behavior of the resonance is shown in Fig. 4. The resonance amplitude becomes constant when the vibration and the damping are in balance. Under a constant Coulomb force, the center position of the resonant oscillation moves. In the energy-conversion process, Coulomb force is applied every half cycle of the vibration, and the resonance amplitude decreases because of the energy scavenging.

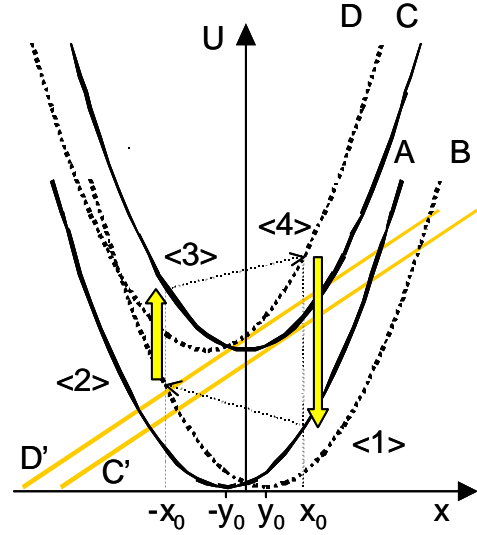


Fig. 5 Potential curves in energy conversion process

### 3. EFFICIENCY ANALYSIS

The efficiency of the vibration-to-electric energy generation is analyzed in three parts: (1) the mechanical-energy conversion of  $C_{var}$ , (2) the charge transportation in the LC tank circuit, and (3) the timing capture.

The mechanical-energy conversion efficiency is analyzed using potential energy curves, as shown in Fig. 5. The conversion process transfers the potential curve in the order of A, B, C, and D.  $y_0$  represents the vibration amplitude, and  $x_0$  represents the balanced displacement of the resonator. Curves C and D include the Coulomb force of the energy conversion. The potential curves are described as

$$U_A = \frac{1}{2}k \cdot (x + y_0)^2, \quad U_B = \frac{1}{2}k \cdot (x - y_0)^2, \quad (2)$$

$$U_C = \frac{1}{2}k \cdot (x - y_0)^2 + \frac{1}{2}q_0 \cdot E_0 \cdot (x - y_0 + z_0), \quad (3)$$

$$U_D = \frac{1}{2}k \cdot (x + y_0)^2 + \frac{1}{2}q_0 \cdot E_0 \cdot (x + y_0 + z_0), \quad (4)$$

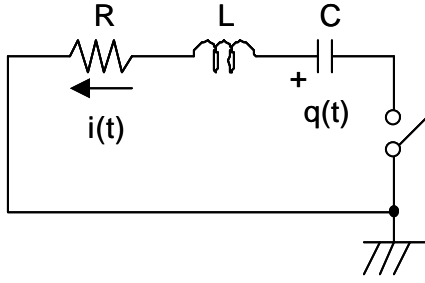


Fig. 6 Equivalent circuit of charge transporter

where  $z_0$  is the distance between the resonator and the electrode. The resonator changes its potential energy along with the points <1>, <2>, <3>, and <4>. Potential transfer from <2> to <3> consumes energy, while the transfer from <4> to <1> generates energy. The difference between energy generation and consumption represents produced energy. The balanced condition and generated power are given by

$$x_0 = \frac{1}{c\mathbf{w}} \cdot \left( ky_0 - \frac{1}{2} q_0 E_0 \right), \quad (5)$$

$$P = f_0 \cdot \frac{2q_0 E_0}{c\mathbf{w}} \cdot \left( (k + c\mathbf{w})y_0 - \frac{1}{2} q_0 E_0 \right), \quad (6)$$

where  $\mathbf{w} = 2pf_0$ . From equation (6), we can see that there is a power-maximizing condition:

$$q_0 E_0 = (k + c\mathbf{w})y_0, \quad (7)$$

$$P_{\max} = \frac{f_0}{c\mathbf{w}} \cdot (k + c\mathbf{w})^2 \cdot y_0^2. \quad (8)$$

Equation (7) determines the optimum design of the variable-capacitive resonator and the power generation system.

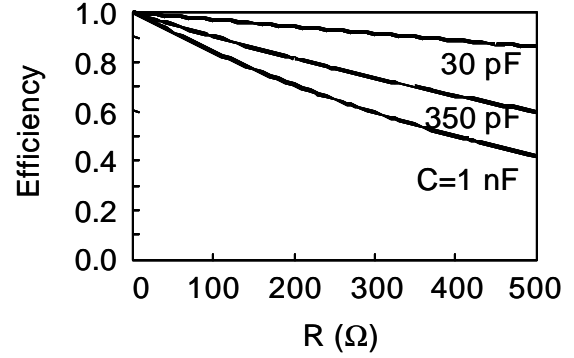


Fig. 7 Efficiency dependence on parasitic resistance in charge transporter

The charge-transportation efficiency is analyzed using the equivalent circuit shown in Fig. 6. The charge transporter in the energy generator has two sets of LC tank circuits. Parasitic elements in the circuit reduce its energy efficiency, so the efficiency is calculated based on an analysis of the LC tank circuits. The circuit equation and the efficiency are described by

$$L \cdot \ddot{q}(t) + R \cdot \dot{q}(t) + \frac{1}{C} \cdot q(t) = 0, \quad (9)$$

$$E_{\text{eff}} = \frac{E_L}{E_L + E_C + E_R} \approx e^{-\frac{pR}{2}\sqrt{\frac{C}{L}}}, \quad (10)$$

where  $E_L$ ,  $E_C$ , and  $E_R$  represent the energy consumption in inductance L, capacitance C and parasitic resistance R, respectively.

Fig. 7 shows the efficiency dependence on the parasitic resistance. The capacitance is 1 nF, 350 pF, or 30 pF, representing the capacitance  $C_{\text{res}}$ , the maximum  $C_{\text{var}}$  capacitance, and the minimum  $C_{\text{var}}$  capacitance of the charge transporter, respectively.

The timing-capture efficiency is assumed to be 100% because the scheme is manually set in the experiment.

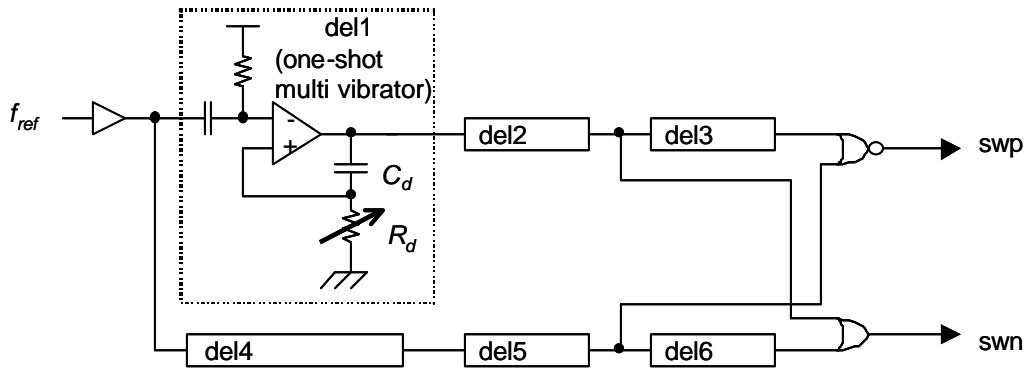


Fig. 9 Timing-capture scheme



Fig. 8 Variable-capacitive resonator

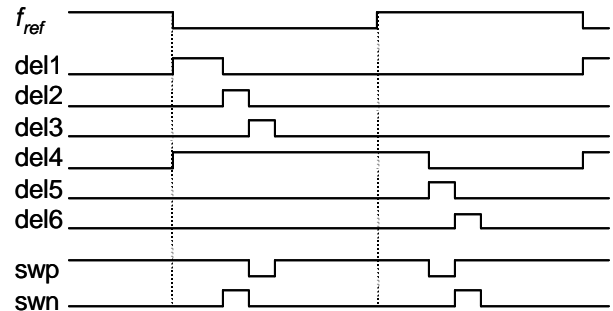


Fig. 10 Timing chart in capture scheme

#### 4. EXPERIMENT AND RESULTS

We fabricated a variable-capacitive resonator and a vibration-to-electric energy generator. The resonator is shown in Fig. 8. A mass of the resonator was put between flat springs. This structure prevented the mass from bending. The initial design settings were an inductance  $L$  of  $820 \mu\text{H}$ , a capacitance  $C_{res}$  of  $1 \text{ nF}$ , a maximum  $C_{var}$  capacitance of  $350 \text{ pF}$  and a minimum  $C_{var}$  capacitance of  $30 \text{ pF}$ . A resonance frequency of the variable capacitance was designed as  $50 \text{ Hz}$ . The timing-capture scheme and its operation are shown in Figs. 9 and 10. The high-signal interval of each delay-block output was manually controlled using a variable resistance  $R_d$ . This made the phases and intervals of the swp and swn signals controllable. External power was supplied only to the timing-capture scheme. The vibration was supplied externally to the resonator by

applying a clock signal,  $f_{ref}$ . The same clock was used for the timing-capture in accordance with the resonance frequency. To reduce the damping, the variable capacitor was set in a low-pressure atmosphere.

As shown in Fig. 11, the resonance frequency was about  $45 \text{ Hz}$ , and the quality factor,  $Q$ , was  $30$ . This means that if the resonator were set on a wall like that used for the measurements shown in Fig. 1, the vibration would have amplitude of  $1 \mu\text{m}$  at  $45 \text{ Hz}$ , so the resonator's amplitude would be  $30 \mu\text{m}$ . The damping coefficient was obtained using  $c = \sqrt{mk} / Q = 0.0471$ . Fig. 12 shows the measured waveforms of the energy converter. The node  $V_{top}$  had a half-cycle sinusoidal wave, and energy was generated during the half cycle. A workload of  $10 \text{ M}\Omega$  was connected to the output,  $V_{out}$ . The measured power was  $120 \text{ nW}$ . From equation (8), the maximum power was estimated to be  $580$

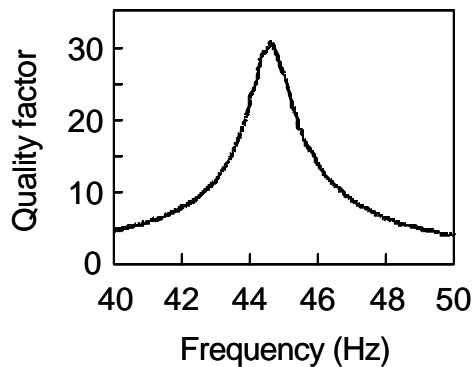


Fig. 11 Response curve of resonator

nW. Therefore, the converter efficiency was 21%, resulting from the combination of 57% mechanical energy efficiency and 37% charge-transporter efficiency. In the charge transporter, this efficiency corresponds to 200- $\Omega$  parasitic resistance or 50- $\Omega$  parasitic resistance with 10-nF parasitic capacitance.

## 5. CONCLUSION

The efficiency of vibration-to-electric energy generation was estimated using a mechanical resonator, a charge transporter, and a timing capture, and then, an optimum design methodology was identified. Experimental results for a vibration-to-electric energy generator using a variable-capacitive resonator showed that the mechanical-resonating efficiency was 57%, and the charge-transportation efficiency was 37%. Vibration energy was successfully converted to electrical energy; the output energy was 120 nW, which corresponds to 21% efficiency.

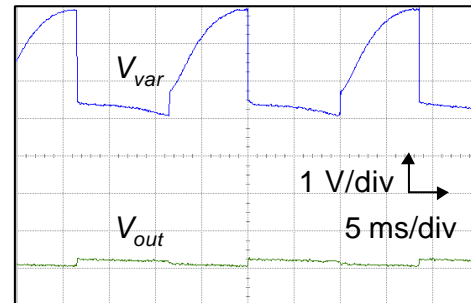


Fig. 12 Measured waveforms of energy converter

## 6. REFERENCES

- [1] R. Tashiro, N. Kabei, T. Shiba, K. Katayama, Y. Ishizuka, F. Tuboi, K. Tsuchiya, "Development of an electrostatic generator that harnesses the motion of a living body," *Journal of the Japan Society of Mechanical Engineers*, vol. C65, no. 634, pp. 268-275 (1999).
- [2] C. B. Williams, R. B. Yates, "Analysis of a micro-electric generator for microsystems," *Proceedings of Transducers '95 / Eurosensors IX*, pp. 369-372 (1995).
- [3] S. Meninger, J. O. Muir-Miranda, R. Amirtherajah, A. P. Chandrakasan, J. H. Lang, "Vibration-to-electric energy conversion," *IEEE Transactions on Very Large Scale Integration (VLSI) Systems*, vol. 9, no. 1, pp. 64-75 (2001).